

SECOND-ORDER SCATTERING INDUCED REFLECTION DIVERGENCE AND NONLINEAR DEPOLARIZATION ON RANDOMLY CORRUGATED SEMICONDUCTOR NANO-PILLARS

G.-R. Lin^{*}, F.-S. Meng, and Y.-H. Lin

Graduate Institute of Photonics and Optoelectronics, Department of Electrical Engineering, National Taiwan University, No. 1 Roosevelt Road, Section 4, Taipei 106, Taiwan, Republic of China

Abstract—Second-order scattering induced reflection divergence and nonlinear depolarization on randomly sub-wavelength corrugated semiconductor nano-pillar surface is observed, which explains the nonlinear transverse electric (TE)/transverse magnetic (TM) mode transformation of the nano-pillar surface reflection with diminishing Brewster angle. The reflected field polarization ratios are increased from 0.12 to 0.65 and from 0.11 to 0.55 under TE- and TM-mode incidences by increasing Si nano-pillar height from 30 to 240 nm. A small-perturbation modeling corroborates the scattering induced second-order polarization transformation to depolarize the reflection from highly corrugated Si nano-pillar surface. The higher field polarization ratio at TE-mode reflection caused by a severer inhomogeneous Si nano-pillars oriented in parallel with surface normal is concluded. With the enlarged field polarization ratio under TM-mode incidence, the angular dependent reflectance spectra with a gradually diminished and shifted Brewster angle from 74° to 45° can be simulated. The nano-roughened surface induced second-order scattering model correlates the diminishing Brewster angle with the surface depolarized reflection.

1. INTRODUCTION

Recently, the sub-wavelength semiconductor anti-reflective and anti-glare structure surface has emerged as an alternative to replace the traditional anti-reflective coatings and has been utilized in versatile

Received 19 March 2011, Accepted 23 May 2011, Scheduled 30 May 2011

* Corresponding author: Gong-Ru Lin (grlin@ntu.edu.tw).

optoelectronic devices [1–7]. In most works, the surface anti-reflection property of the nano-roughened structure was typically realized as a multi-layered model with gradually changed refractive index induced by different air-Si mixture compositions [8]. In addition, the investigation of light scattering from the roughened anti-glare surface has caused great interests in scientific researches [9–16]. In 1967, the surface depolarization on the backscattered light from either the disordered metallic or inhomogeneous dielectric surfaces under a linearly polarized incidence at different angles were experimentally characterized without theoretical modeling [9]. Later on, the works described the multiple light scattered from the anti-glare surface with irregularly distributed spherical nano-particles with Mie scattering theory [17,18]. The depolarization is attributed to the multiple scattering with the degree of depolarization seriously enhanced by increasing reflections from sub-surface of the roughened metallic or inhomogeneous dielectrics [19]. It was preliminarily assumed that the volume scattering within the inhomogeneous dielectrics plays an important role on the depolarization phenomenon [20], assuming the depolarized reflection under the linearly polarized incidence is a function independent with the surface roughness and the scattering angle [20]. Until 1975, both the surface and the sub-surface scattering effects were taken into consideration via the use of single-surface Kirchhoff method [21]. The derivation was reported to coincide with the preliminary observation [22] that the backscattered light is surface-roughness dependent, whereas the depolarization contributed by surface corrugation is negligible. Nonetheless, an extinction theorem was subsequently to correlate the depolarized reflectance with the surface corrugation without giving experimental evidence [23]. Under a linearly polarized light incidence into nano-scale roughened sub-wavelength semiconductor anti-reflective/anti-glare structure surface, such a surface-roughness dependent or independent reflection depolarization was still left as an uncertainty until now. The latter quantitative analyses on the scattering beam divergence and the incident-mode dependent reflection depolarization with the aspect ratio of the nano-roughened semiconductor surface were seldom correlated with these dialectical modeling works up to now. A latter experiment in 1994 also reported that the incident light with specific polarization was found to lose its polarization in randomized multiple scattering surface [24]. Some scientists have ever provided conceptual description that the polarized light undergoes serious scattering and multiple reflections within the inhomogeneous dielectrics, where the induced dipoles suffer from the superposition of numerous unrelated optical fields to result in the completely depolarized reflection [25].

Even though, the depolarization of light in such an inhomogeneously nano-corrugated medium is still not quantitatively analyzed and completely elucidated due to the complex numerical calculation of the randomly multiple scattering.

This work discusses the disordered nano-pillar roughened Si surface with pillar-height dependent divergence of reflection beam and reduction of polarization ratio, which are analyzed and elucidated by using a multiple scattering model based on the Ewald-Oseen extinction theorem numerically derived by Nieto-Vesperinas calculation. The diagnosis of a set of Si nano-pillar samples with lengthening pillar heights is numerically simulated to confirm the observed variation on the degree of depolarization and shifting Brewster angle, and its correlation with the nano-pillar height dependent surface scattering. The multiple scattering is characterized by measuring the scattered reflection intensity versus the divergent angle from Si nano-pillar surface. The shift and disappearance of Brewster angle in angular reflectance spectrum and its correlation with depolarization are explained through modeling.

2. EXPERIMENT

The Ni nano-dots covered SiO₂ nano-mask assistant dry-etching method was utilized to fabricate the semiconductor anti-reflective nano-pillar on n-type (100)-oriented Si substrate surface with different pillar heights [26]. In the beginning, we deposited a Ni film with 50 nm thick on the 200Å-thick SiO₂ coated Si substrate by using an e-beam evaporator, and the Ni deposition rate is 0.1Å/s. The self-aggregation of Ni nano-dots was occurred by employing the rapid thermal annealing process at 850°C for 22 s under the N₂ flowing gas, the area density of Ni nano-dots on SiO₂/Si substrate is $5 \times 10^{11} \text{ cm}^{-2}$.

In the dry-etching process, a planar-type inductively coupled plasma enhanced reactive ion etching system (ICP-RIE) with ICP/bias power of 100/50 watts was used to adjust the Si nano-pillar height. During the etching process, the CF₄/Ar ratio of the gas mixture was 40/40 SCCM and the chamber pressure was 0.66 Pa. Simultaneously, the Si nano-pillar height was controlled by detuning the fluencies of the oxygen gas in the ICP-RIE chamber. The Si nano-pillar based anti-reflective surface with pillar height from 30 to 240 nm, changing pedestal width from 20 to 60 nm, altering sidewall slope (the ratio of the nano-pillar height to the half-pedestal width) from 2 to 7 were synthesized by detuning the etching time between 5 to 7 min.

3. RESULTS AND DISCUSSION

To measure the divergence of the scattered reflection-beam from Si or Si nano-pillar surface, a CW Nd:YAG laser (532 nm) with output power of 10 mW and a linear polarizer with extinction ratio up to 10000 : 1 are used to produce the TE and TM-mode light sources. The incidence angle is fixed at 20° in every measurement, and the distance between the sample and the power meter is 7 cm. The reflected power is collected by adding a pin hole with diameter of $250\ \mu\text{m}$ prior to the power sensor head. The scattering reflection effect of the Si nano-pillar surface is characterized by concentrically scanning the power sensor related to the reflected beam axis with the use of a rotating stage, giving the scattered light intensity as a function of rotating angle in the vertical and the horizontal direction.

A significant multiple scattering accompanied with a serious divergence reflection-beam is observed from the Si nano-pillar surface. Under TE and TM-mode incidences on Si nano-pillar and Si wafer surface, the scattered reflection-beam intensity versus the divergent angle are analyzed to characterize the degree of scattering. For example, the Figures 1(a) and 1(b) demonstrate the three-dimensional

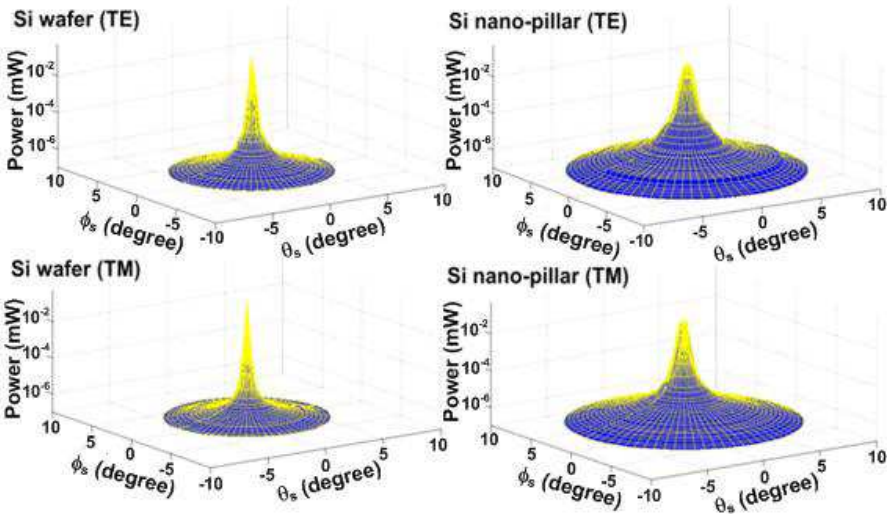


Figure 1. The mode dependent divergence and scattering of the reflected beam from Si wafer (left) and 240-nm long Si nano-pillar (right) surfaces under TE- (upper) and TM-mode (lower) incidences, respectively.

contour maps of the angular dependent scattered reflection intensity from the surfaces of the flat Si wafer and the Si nano-pillar sample with a pillar length of 240 nm, respectively. A purely Gaussian distribution sustains for the surface reflection from the unprocessed Si wafer, whereas the reflection from Si nano-pillar surface reshape itself to shown a degraded Gaussian function with the divergent angle. Not only the central part of the reflection beam broadens its angular distribution from 0.33° (for Si wafer) to 0.9° (for Si nano-pillar surface), but also the scattered pedestal of the reflection beam greatly diverges from 4° (for Si wafer) to 14° (for Si nano-pillar surface). In particular, the divergent angle of the surface reflection from Si nano-pillar is much broader than that from the Si wafer, and the TE-mode incidence induces a larger divergence than TM-mode incidence. These results interpret that the linearly and orthogonally polarized incidences could suffer from different multiple scattering effects in the inhomogeneous and nano-roughened material surface to cause the varying degree of depolarization.

Although it was preliminarily observed that the inhomogeneous dielectric material with roughened surface enables the depolarization of the incident light at all angles of incidence [27], where the multiple scattering was assumed to play an important role on such a depolarization effect [19], the quantitative analysis on the aspect-ratio dependent depolarization of the nano-scaled semiconductor nano-pillar surface has not yet been investigated in detail. During our analysis, the reflected polarization ratios P_{TE} (at TE-mode incidence) and P_{TM} (at TM-mode incident) are defined as $(I_{TE}/TE - I_{TM}/TE)/(I_{TE}/TE + I_{TM}/TE)$ and $(I_{TM}/TM - I_{TE}/TM)/(I_{TM}/TM + I_{TE}/TM)$, respectively. The sub-wavelength nano-pillar surfaces with different thickness are measured under linearly polarized laser illumination with a schematic diagram shown in Figure 2. A CW Nd:YAG laser and a linear

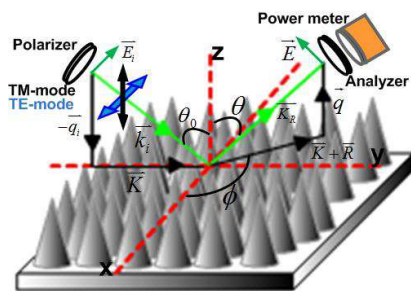


Figure 2. Diagnostic setup for analyzing the scrambled polarization state of reflection from semiconductor nano-pillar surface.

polarizer are combined to be the light source with TE- and TM-mode incidences, the incident angle is about 20° . An analyzer is inserted in front of the power sensor to analyze the polarization distribution of the reflected beam. The polarization ratio of the reflected beam from the Si nano-pillar sample is detected by rotating the axes of the polarizer and the analyzer from parallel to orthogonal (from 0° to 90°) condition. The depolarized reflectance data of sub-wavelength nano-pillar based anti-reflective/anti-glare surface with different geometrical factors have been measured as a function of the analyzer angle. The example scanning-electron microscopic image of Si nano-pillar with pillar height of 150 nm and the experimental results of angular dependent normalized reflection intensity under TE and TM-mode incidences versus nano-pillar height are demonstrated in Figures 3(a) and 3(b). For TE-mode and TM-mode incidences, the nano-pillar corrugated surface reflectance is plotted as a function of the angular difference between the polarizer and analyzer axes. The reflectance of an unprocessed Si wafer completely diminishes when the deviated angle between polar and analyzer gradually enlarges to 90° , whereas the Si nano-pillar roughened surface reveals an enlarged reflectance with increasing nano-pillar height.

The higher Si nano-pillar inevitably leads to the worse degradation on the reflected polarization ratio, which is attributed to the serious scattering within the higher aspect-ratio Si nano-pillar corrugated surface. Such an anomalous reflectance induces a

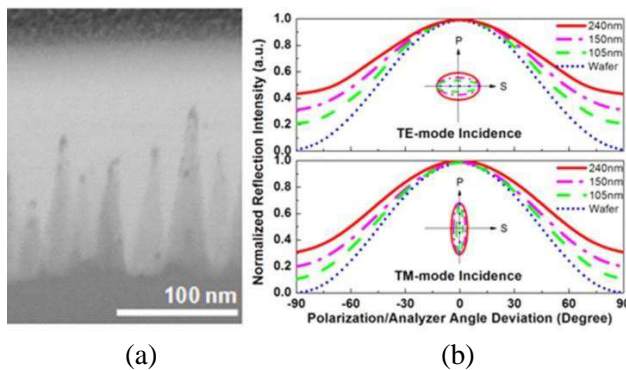


Figure 3. (a) the SEM images of Si nano-pillar samples with different pillar length; (b) the normalized reflection intensity of the Si nano-pillar corrugated surface as a function of the angular difference between polarizer/analyzer axes under TE-mode (upper) and TM-mode incidence (lower).

partially polarization-mode transformation to scramble the reflected polarization, in which the degree of polarization is dependent with the original polarization mode. The TE-mode incidence induces a severer degradation on the reflected polarization than the TM-mode incidence does. With an enlarging nano-pillar height, the lower polarization ratio of the polarized reflectance is observed to degrade when comparing with that of the original incidence. If we plot the polarization states of the reflected beam, it is clearly shown that both the TE- and TM-mode incidences induce the polarization scrambling effect on the reflection from the surface corrugated by randomly distributed Si nano-pillars. However, the TE-mode suffers from a more significant depolarization effect than that of the TM-mode, as shown in Figure 3.

Both the reflected intensity polarization ratios under TE- and TM-mode incidences remain as high as 97% when the pillar height is smaller than 30 nm, which is not influenced by the Si nano-pillar roughened surface with a small corrugation. Nevertheless, the intensity polarization ratio of P_{TM} under TM-mode incidence is degraded from 97.5% to 53%, respectively, as the Si nano-pillar height increases from 30 to 240 nm (see Figure 4). In contrast, the P_{TE} obtained under TE-mode incidence decays from 96.8% to 40% after suffering from a severer depolarization during reflection. Since the inhomogeneous Si nano-pillar structure causes a different surface scattering effect [28] on the TE- and TM-mode incidences, which inevitably results in a deviation on the reflected depolarization as the surface corrugation becomes significant. In experiment, we observe that the depolarized reflection from the Si nano-pillar roughened surface is strongly related to the nano-pillar length, which can be correlated to the simulation on the corrugated surface scattering

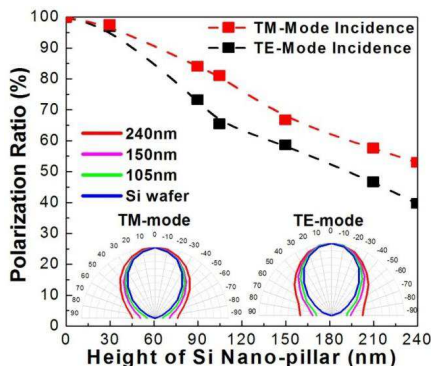


Figure 4. The intensity polarization ratio of nano-pillar corrugated surface as a function of different Si nano-pillar heights.

previously established by Nieto-Vesperinas [23]. The depolarization from the roughened semiconductor surface enhances with lengthening nano-pillar height due to the enlarged scattering and transformation between the orthogonal polarization-modes in reflection.

To further investigate the depolarization of the electromagnetic wave scattered from Si nano-pillar roughen surface, the Nieto-Vesperinas calculation based on the Ewald-Oseen extinction theorem is introduced [21]. Assume that a linear polarized wave $E_i(r)$ with wave vector $\vec{k}_i = (\vec{K}, -q_i)$ is incident on the sub-wavelength nano-pillar surface with a surface profile of $z = \alpha D_R(r)$, where $D_R(r)$ represents the corrugation function and α denotes the nano-pillar height dependent parameter to describe the roughness of the nano-pillar surface. The optical field of the incident laser beam is described as $\vec{E}_i(\vec{r}) = \vec{E}_0 \exp[i(\vec{K} \cdot \vec{R} - q_i z)]$ with $\vec{E}_0 = (E_{01}, E_{02}, E_{03})$ denoting a constant field vector. Several parameters are introduced to obtain the scattered field from the nano-pillar roughened semiconductor surface, the $\vec{k}_R = (\vec{K} + \vec{R}, q_i)$ is given as the propagating vector of the reflected field with $\vec{R} = (-R_1, R_2, 0)$ and $\vec{k} = (\vec{K} + \vec{R}, -q)$. The \vec{a}_{TE} and \vec{a}_{TM} denote two orthogonal unit vectors of TE and TM polarized waves corresponding to the scattering plane, as described by $\vec{a}_{TE} = (\vec{K} + \vec{R})/|\vec{K} + \vec{R}| \times \vec{z}$ and $\vec{a}_{TM} = \vec{a}_{TE} \times \vec{k}_R/k_i$. With the $E_{02} = E_{03} = 0$ assumed TE-incidence, the TE- and TM-component of the optical field are denoted as $E_{TE/TE}(\vec{R})$ and $E_{TM/TE}(\vec{R})$, respectively. For TM-incidence, $E_{01} = 0$, and the TE- and TM-component of the scattered electric field are denoted as: $E_{TE/TM}(\vec{R})$ and $E_{TM/TM}(\vec{R})$. With the small-perturbation approximation derived in the previous work [23], the nano-pillar surface shape dependent scattering and depolarization on the four optical field components are expressed as below, in which the incident and reflected angles are replaced by Cartesian coordinate parameters.

$$E_{TE/TE}(\vec{R}) = -q_i E_{01} \left\{ \left[\frac{1}{q_i} \delta(\vec{R}) - 2i\alpha D_R - 2\alpha^2 q (D_R * D_R) \right] \frac{(K + R_2)}{[R_1^2 + (K + R_2)^2]^{1/2}} - 2\alpha^2 \frac{R_1}{q} (D_R * D_R) \vec{k} \cdot \vec{a}_{TE} \right\} \quad (1)$$

$$E_{TM/TE}(\vec{R}) = q_i E_{01} \left\{ \left[\frac{1}{q_i} \delta(\vec{R}) - 2i\alpha D_R - 2\alpha^2 q (D_R * D_R) \right] \left(\frac{q R_1}{k_i [R_1^2 + (K + R_2)^2]^{1/2}} \right) + \left[i\alpha D_R R_1 + \alpha^2 q_i E_{01} \frac{R_1^2}{q k_i^2} (D_R * D_R) \right] \frac{2[R_1^2 + (K + R_2)^2]^{1/2}}{q k_i} - 2\alpha^2 \frac{R_1}{q} (D_R * D_R) \vec{k} \cdot \vec{a}_{TM} \right\} \quad (2)$$

$$E_{TE/TM}(\vec{R}) = -E_{02} \frac{k_i^2}{q_i} \left\{ \left[\frac{1}{q_i} \delta(\vec{R}) - 2i\alpha D_R - 2\alpha^2 q (D_R * D_R) \right] \frac{R_1}{[R_1^2 + (K + R_2)^2]^{1/2}} - 2\alpha^2 \frac{R_2}{q} (D_R * D_R) \vec{k} \cdot \vec{a}_{TE} \right\} \quad (3)$$

$$E_{TM/TM}(\vec{R}) = \frac{E_{02} k_i^2}{q_i} \left\{ \left[\frac{1}{q_i} \delta(\vec{R}) - 2i\alpha D_R - 2\alpha^2 q (D_R * D_R) \right] \frac{q(K + R_2)}{k_i [R_1^2 + (K + R_2)^2]^{1/2}} + 2\alpha^2 \frac{R_2}{q} (D_R * D_R) \vec{k} \cdot \vec{a}_{TM} \right\} \quad (4)$$

The field polarization ratios of the scattered optical reflectance under TE- and TM-mode incidences are defined as $E_{TM/TE}(\vec{R})/E_{TE/TE}(\vec{R}) = [I_{TM/TE}(\vec{R})/I_{TE/TE}(\vec{R})]^{1/2}$ and $E_{TE/TM}(\vec{R})/E_{TM/TM}(\vec{R}) = [I_{TE/TM}(\vec{R})/I_{TM/TM}(\vec{R})]^{1/2}$, respectively. By using the parameters: $\cos \phi = R_1/[R_1^2 + (K + R_2)^2]^{1/2}$, $\sin \phi = (K + R_2)/[R_1^2 + (K + R_2)^2]^{1/2}$, $K = k_i \sin \theta_0$, $q_i = k_i \cos \theta_0$ and $q = k_i \cos \theta$. The simulated results can be obtained. As a result, the Figure 5 demonstrates the simulated and the measured field polarization ratios of the Si nano-pillar with varied nano-pillar lengths under TE- and TM-mode incidences, which increase from 0.12 to 0.65 under TE-mode incidence and from 0.11 to 0.55 under TM-mode incidence by enlarging nano-pillar length from 30 to 240 nm. According to the theoretical simulation, the field polarization ratio closely correlates with the surface profile through αD_R by the second-order expansion of the optical field. Both the experimental and simulated results are qualitatively resembled to the Rayleigh-Fano approach [29], suggesting that the reflected depolarization occurred at corrugated surface is a second-

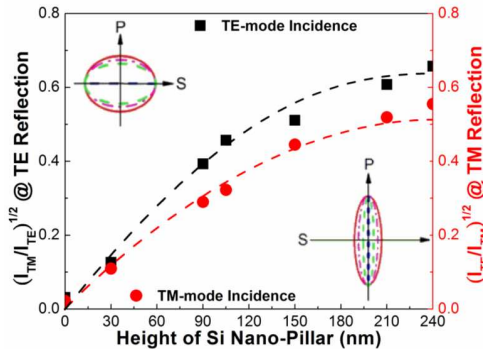


Figure 5. The field polarization ratio of Si nano-pillar with varied nano-pillar length under TE- and TM-mode incidences.

order scattering effect under small-perturbation approximation. The linearly polarized optical incidence is perturbed when impinging on the roughened surface, such that the scattered reflection changes its polarization from linear to elliptical one. Increasing the Si nano-pillar length would lead to a more corrugated surface with enlarging the field polarization ratio. The depolarization is indeed the second-order effect of the field expansion due to the nano-pillar surface corrugation with the perturbation expansion in powers of α , as obtained from the modeling. The simulation results also verify the fact of a larger depolarization happened for TE-mode incidence due to the existence of second term in Equation (2). For TM-mode incidence, the reflected optical wave depolarizes into a second-order TE-mode scattered wave due to the appearance of the third term in Equation (4). As evidence, the lower field polarization ratio is obtained under TM-mode incidence, whereas the TE-mode incidence with its polarization orthogonal to the orientation of the vertically aligned Si nano-pillars inevitably suffers from a severer depolarization.

Since the TM-mode incidence provides a larger scalar product with the internal displacement field within these Si nano-structures than the TE-mode. That is, the optical field component within the randomly corrugated surface experiences such nano-structures more like an unprocessed bulk Si wafer for TM-mode case. Under the presence of an incident optical wave with its polarization in parallel with the perpendicularly aligned nano-pillars, more bound electrons within Si atoms undergo the driving force for remaining its dielectric permittivity less deviated from that in bulk case. In contrast, the TE-mode incidence interacts with fewer bounded electrons but penetrates a deeper air-Si mixed structure to induce a severer scattering effect. Consequently, the reflectance behavior of TM-mode incidence is less different from the bulk Si case, whereas the TE-mode incidence faces a more significant scattering and depolarization problem.

In addition, such a polarization scrambling effect due to the Si nano-pillar induced second-order scattering process also causes a Brewster angle diminishing phenomenon under TM-mode incidence, as shown in Figure 6. According to the measured results of depolarization phenomenon which occurs in Si nano-pillar roughened surface, the gradually shifted and diminishing Brewster angle is expected and attributed to the depolarized reflection from the highly corrugated Si nano-pillar surface with gradually enlarged aspect-ratio. The angular dependent reflectance spectra with a gradually shifted Brewster angle from 74° to 45° can be simulated with the enlarged field polarization ratio under TM-mode incidence from 0.11 to 0.55. The experimental results show that the Brewster angle phenomenon is eventually

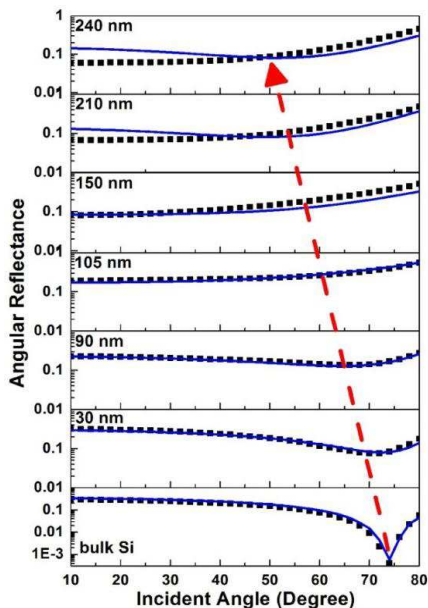


Figure 6. The experimental (black dotted) and simulated (blue solid) reflectance from the Si nano-pillar corrugated surface as a function of the incident angle.

disappeared from the angular reflectance of Si nano-pillar surface with pillar height up to 240 nm. The significant deviation between the experimental and simulated curves of the angular reflectance spectra happened at nearly grazing-angle incidence for all samples. In particular, a similar deviation was observed at nearly Brewster angle for longer nano-pillar samples, which is caused by the larger surface scattering effect [30] than expected. In this case, the reflected beam becomes too divergent to be completely collected by the detecting optics, and the scattering of TM-mode is severer than that predicted by the small-perturbation model. As the field polarization ratio increases, the Brewster angle shifts toward small angle and the Brewster angle phenomenon related reflection dip at angular reflectance spectrum gradually disappears. With a critical nano-pillar height of 150 nm, the depolarization effect dominates the reflected beam in which a part of the original incidence with its specific polarization transferring to another polarization state. Therefore, the TM-mode incidence dependent Brewster angle phenomenon diminishes when the pure TM-mode reflection is partially depolarized to a mixed TE+TM polarization-mode output.

4. CONCLUSION

In conclusion, the depolarized reflection of the Si nano-pillar roughened surface with different corrugation factor is investigated. The central part of the reflection beam broadens its angular distribution from 0.33° (for Si wafer) to 0.9° (for Si nano-pillar surface), but also the scattered pedestal of the reflection beam greatly diverges from 4° (for Si wafer) to 14° (for Si nano-pillar surface). The surface depolarization with field polarization ratios increased from 0.12 to 0.65 and 0.11 to 0.55 under TE- and TM-mode incidences, respectively, are observed by enlarging nano-pillar height from 30 to 240 nm. The severer corrugated surface results in a worse depolarization, which is ascribed to the stronger scattering induced polarization mode transformation. Therefore, the diminish on the TM-mode incidence dependent Brewster angle phenomenon is expected when the pure TM-mode reflection is partially depolarized to mixed TE+TM mode output. In addition, the lower field polarization ratio is obtained under TM-mode incidence, whereas the more serious depolarization under TE-mode incidence by the enhanced scattering in the nano-pillar structure is confirmed. In contrast to the TE-mode incidence, the less depolarized reflection under TM-mode incidence owing to the second-order scattering term occurred in the reflected orthogonal polarization can be obtained by small-perturbation simulation. The angular dependent reflectance spectra with a gradually shifted Brewster angle from 74° to 45° can be simulated with the enlarged field polarization ratio under TM-mode incidence. As the field polarization ratio increases, the Brewster angle shifts toward small angle and the related reflection dip at angular reflectance spectrum gradually disappears.

ACKNOWLEDGMENT

The work was financially supported by National Science Council and National Taiwan University under grants NSC98-2221-E-002-023-MY3, NTU98R0062-07 and NSC 100-2623-E-002-002-ET.

REFERENCES

1. Kanamori, Y., M. Sasaki, and K. Hane, "Broadband antireflection gratings fabricated upon silicon substrates," *Opt. Lett.*, Vol. 24, 1422–1424, 1999.
2. Hattori, H., "Anti-reflection surface with particles coating deposited by electrostatic attraction," *Adv. Mater.*, Vol. 13, No. 1, 51–54, 2001.
3. Lee, C., S. Y. Bae, S. Mobasser, and H. Manohara, "A novel

- silicon nanotips antireflection surface for the micro sun sensor,” *Nano Lett.*, Vol. 5, 2438–2442, 2005.
4. Peng, K. Q., Y. Xu, Y. Wu, Y. Yan, S. T. Lee, and J. Zhu, “Aligned single-crystalline Si nanowire arrays for photovoltaic applications,” *Small*, Vol. 1, 1062–1067, 2005.
 5. Diedenhofen, S. L., G. Vecchi, R. E. Algra, A. Hartsuiker, O. L. Muskens, G. Immink, E. P. A. M. Bakkers, W. L. Vos, and J. G. Rivas, “Broad-band omnidirectional antireflection coatings based on semiconductor nanorods,” *Adv. Mater.*, Vol. 21, 973–978, 2009.
 6. Ding, B., M. Bardosova, I. Povey, M. E. Pemble, and S. G. Romanov, “Engineered light scattering in colloidal photonic heterocrystals,” *Adv. Funct. Mater.*, Vol. 20, 853–860, 2010.
 7. Wan, D., H. L. Chen, T. C. Tseng, C. Y. Fang, Y. S. Lai, and F. Y. Yeh, “Antireflective nanoparticle arrays enhance the efficiency of silicon solar cells,” *Adv. Funct. Mater.*, Vol. 20, 3064–3075, 2010.
 8. Huang, Y.-F., S. Chattopadhyay, Y.-J. Jen, C.-Y. Peng, T.-A. Liu, Y.-K. Hsu, C.-L. Pan, H.-C. Lo, C.-H. Hsu, Y.-H. Chang, C.-S. Lee, K.-H. Chen, and L.-C. Chen, “Improved broadband and quasi-omnidirectional anti-reflection properties with biomimetic silicon nanostructures” *Nature Nanotechnol.*, Vol. 2, 770–774, 2007.
 9. Renau, J., P. K. Cheo, and H. G. Cooper, “Depolarization of linearly polarized EM waves backscattered from rough metals and inhomogeneous dielectrics,” *J. Opt. Soc. Am.*, Vol. 57, 459–461, 1967.
 10. Muskens, O. L., S. L. Diedenhofen, M. H. M. V. Weert, M. T. Borgström, E. P. A. M. Bakkers, and J. G. Rivas, “Epitaxial growth of aligned semiconductor nanowire metamaterials for photonic applications,” *Adv. Funct. Mater.*, Vol. 18, 1039–1046, 2008.
 11. Wang, M.-J., Z.-S. Wu, and Y.-L. Li, “Investigation on the scattering characteristics of gaussian beam from two dimensional dielectric rough surfaces based on the kirchhoff approximation,” *Progress In Electromagnetics Research B*, Vol. 4, 223–235, 2008.
 12. Du, Y. and B. Liu, “A numerical method for electromagnetic scattering from dielectric rough surfaces based on the stochastic second degree method,” *Progress In Electromagnetics Research*, Vol. 97, 327–342, 2009.
 13. Lin, Z. W., X. J. Zhang, and G. Y. Fang, “Theoretical model of electromagnetic scattering from 3D multi-layer dielectric

- media with slightly rough surfaces,” *Progress In Electromagnetics Research*, Vol. 96, 37–62, 2009.
14. Durian, D. J., D. A. Weitz, and D. J. Pine, “Multiple light-scattering probes of foam structure and dynamics,” *Science*, Vol. 252, 686–688, 2010.
 15. Kim, K. S., S. M. Kim, H. Jeong, M. S. Jeong, and G. Y. Jung, “Enhancement of light extraction through the wave-guiding effect of ZnO sub-microrods in InGaN blue light-emitting diodes,” *Adv. Funct. Mater.*, Vol. 20, 1076–1082, 2010.
 16. Huang, F., D. Chen, X. L. Zhang, and R. A. Caruso, “Dual-function scattering layer of submicrometer-sized mesoporous TiO₂ beads for high-efficiency dye-sensitized solar cells,” *Adv. Funct. Mater.*, Vol. 20, 1301–1305, 2010.
 17. Handapangoda, C. C., M. Premaratne, and P. N. Pathirana, “Plane wave scattering by a spherical dielectric particle in motion: A relativistic extension of the Mie theory,” *Progress In Electromagnetics Research*, Vol. 112, 349–379, 2011.
 18. Liang, D., P. Wu, L. Tsang, Z. Gui, and K.-S. CHen, “Electromagnetic scattering by rough surfaces with large heights and slopes with applications to microwave remote sensing of rough surface over layered media,” *Progress In Electromagnetics Research*, Vol. 95, 199–218, 2009.
 19. Chy’lek, P., G. W. Grams, and R. G. Pinnick, “Light scattering by irregular randomly oriented particles,” *Science*, Vol. 193, 480–482, 1976.
 20. Leader, J. C. and W. A. J. Dalton, “Bidirectional scattering of electromagnetic waves from the volume of dielectric materials,” *J. Appl. Phys.*, Vol. 43, No. 7, 3080–3090, 1972.
 21. Wilhelmi, G. J., J. W. Rouse, and A. J. Blanchard, “Depolarization of light back scattered from rough dielectrics,” *J. Opt. Soc. Am.*, Vol. 65, 1036–1042, 1975.
 22. Rouse, J. W., “The effect of the subsurface on the depolarization of rough-surface backscatter,” *Radio Sci.*, Vol. 7, 889–895, 1972.
 23. Vesperinas, M. N., “Depolarization of electromagnetic waves scattered from slightly rough random surfaces: A study by means of the extinction theorem,” *J. Opt. Soc. Am. A*, Vol. 72, 539–547, 1982.
 24. Rojas-Ochoa, L. F., D. Lacoste, R. Lenke, P. Schurtenberger, and F. Scheffold, “Depolarization of backscattered linearly polarized light,” *J. Opt. Soc. Am. A*, Vol. 21, 1799–1804, 2004.
 25. Hecht, E., *Optics*, Addison Wesley, San Francisco, 2002.

26. Lin, G.-R., Y. C. Chang, E. S. Liu, H. C. Kuo, and H. S. Lin, "Low refractive index Si nanopillars on Si substrate," *Appl. Phys. Lett.*, Vol. 90, 181923, 2007.
27. Bicout, D., C. Brosseau, A. S. Martinez, and J. M. Schmitt, "Depolarization of multiply scattered waves by spherical diffusers: Influence of the size parameter," *Phys. Rev. E*, Vol. 49, 1767–1770, 1994.
28. Mittal, G. and D. Singh, "Critical analysis of microwave scattering response on roughness parameter and moisture content for periodic rough surfaces and its retrieval," *Progress In Electromagnetics Research*, Vol. 100, 129–152, 2010.
29. Valenzuela, G. R., "Depolarization of EM waves by slightly rough surfaces," *IEEE Trans. Antennas Propag.*, Vol. 15, 552–557, 1967.
30. Guo, L.-X., A.-Q. Wang, and J. Ma, "Study on EM scattering from 2-D target above 1-D large scale rough surface with low grazing incidence by parallel MoM based on PC clusters," *Progress In Electromagnetics Research*, Vol. 89, 149–166, 2009.